Physica B: Condensed Matter 552 (2019) 209–213

Contents lists available at ScienceDirect

Physica B: Condensed Matter

journal homepage: www.elsevier.com/locate/physb

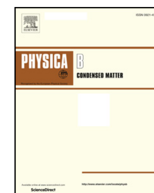

The formation and characterization of optical waveguide in Nd:YLF crystal by 4.5-MeV Si ion implantation

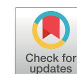

Xiao-Xiao Song, Yao Wang, Song Li, Chuan-Lei Jia*

School of Physical Science and Technology, China University of Mining and Technology, Xuzhou 221116, PR China

ARTICLE INFO

Keywords:
Ion irradiation
Waveguide
Photoluminescence
Nd:YLF

ABSTRACT

The planar waveguides have been fabricated in Nd:YLF crystals by Si implantation. The guiding properties of Si-implanted waveguide are evaluated by the prism-coupling technique and reflectivity calculation method (RCM), exhibiting good confinement and monomode behavior at 632.8 nm. The investigation of the photoluminescence (PL) measurement demonstrates that the luminescence characteristics of the Nd^{3+} ions are not significantly altered by the Si ions irradiation process, whereas the up-conversion (UC) luminescence intensity can be effectively improved. Based on the pump-power-dependent fluorescence, the possible emission mechanism in Nd:YLF is proposed.

1. Introduction

$YLiF_4$ (YLF) crystal is an outstanding laser material in advanced photonics and nonlinear optics owing to its remarkable features such as low effective phonon energy and good chemical stability [1]. Among the various possibilities, rare-earth-doped YLF have been widely studied as promising materials for a broad range of laser operation, acousto-optic device and laser amplifiers [2–6]. So far, the trivalent Nd^{3+} ion has attracted significant attentions because of its unique orbital structures including 17 spectroscopic terms and 41 energy levels which can offer multiple channels for fluorescence emissions. Moreover, the trivalent Nd^{3+}-doped host matrices have received increasing interests as active media to obtain near-infrared (NIR) lasers operating around 1064 nm [6]. Especially, Nd:YLF crystal is much attractive in integrated optoelectronic devices and diode-pumped lasers thanks to its natural combination of the unique laser performances of Nd^{3+} and excellent nonlinear optical properties of YLF crystal [7–9]. In many respects, the miniaturization of lasers into monolithic devices is necessary since the integrated photonic circuits are often conceived as planar surface structure with components that have linear dimensions of micron size. For those potential applications, the design and fabrication of miniaturized waveguide is especially important to obtain high photon density and optical conversion efficiencies. Research on optical waveguides is developing continuously in view of the increasing demand of compact devices. Up to now, various techniques have been developed to fabricate optical waveguides including femtosecond laser writing, ion irradiation, metal diffusion and ion exchange [10–13]. Among those, ion irradiation also ion implantation, as a powerful technique for materials modification, has been demonstrated to be an effective and competitive way to produce high-quality waveguides in more than 100 optical materials for its features of controllability and reproducibility [14]. Additionally, it has been proved that ion irradiation is also useful for modulating the optical and spectral properties of laser materials. So far, optical waveguides using energetic light ions (H, He) or swift heavy ions (C, O, Si) have been extensively investigated [15–20]. Compared with light-ion implantation, low-dose heavy ions implantation can induce large refractive index variations in the implanted region. In 2007, Tan et al. reported their work on the C-implanted Nd:YLF waveguides with fluences of $\sim 10^{15}$ [15]. Recent research reveals that heavy ions Si implantation could form waveguide structures efficiently on the surface of optical materials with much lower doses $\sim 10^{14}$ [18,21]. According to the literature on H— or C—ion-implanted Nd:YLF waveguides, the issues mainly focused on the characterizations of the guiding properties. To our knowledge, the optical waveguides formation in Nd:YLF crystal by Si ions implantation have not been reported. The effect of irradiation on the optical and spectral properties of Nd:YLF has not been fully explored. Moreover, the demand for better performance in high-power application for the different laser concepts in Nd:YLF is ongoing. Thus a clear understanding of the effect of ion irradiation is essential to research on the manipulation of optical and spectral properties of Nd:YLF crystals. Here, in order to explore the possibility of a single-mode planar waveguide formed in the Nd:YLF crystal and to study the photoluminescence features of Nd^{3+} after ion implantation, the 4.5-MeV Si ions irradiation in

* Corresponding author.
E-mail address: jiachl@cumt.edu.cn (C.-L. Jia).

https://doi.org/10.1016/j.physb.2018.10.017
Received 13 September 2018; Received in revised form 7 October 2018; Accepted 8 October 2018
Available online 10 October 2018
0921-4526/ © 2018 Elsevier B.V. All rights reserved.

Nd:YLF crystals was carried out at the 1.7 MV tandem accelerator of Peking University. The optical analyses of the waveguide such as refractive index profile and propagation mode distribution as well as fluorescence properties of Nd^{3+} are discussed in detail.

2. Experimental details

A set of z-cut Nd:YLF single crystals (doped with 1.0 at% Nd^{3+}) were implanted by 4.5-MeV Si ions with fluences of $1.0 \times 10^{14}\,cm^{-2}$. All samples were optically polished and cleaned before implantation. During implantation, the samples were titled by 7° from the direction of the ion beam to minimize the channeling effect. The prism-coupling method was used to observe guiding modes of the Nd:YLF planar waveguides with a Model 2010 prism coupler (Metricon 2010, USA) at a wavelength of 632.8 nm with transverse electric (TE) polarization. The accuracy of prism coupler measurements is ± 0.0001. The error is better than 0.001 by uncertainties in the measuring prism angle and index. The reconstruction of refractive index was performed by a program code based on RCM [22]. The electric field distribution of the measured TE mode was obtained to investigate confinement in the implanted waveguides. The UC and NIR emission spectra of the implanted waveguide and the bulk of Nd:YLF crystal were measured on an Edinburgh FS5 spectrometer under excitation with an 808-nm diode laser.

3. Results and discussion

In the past few decades, the prism coupling technique has been well developed to investigate optical properties of many kinds of materials, including dielectric thin films and bulk crystals. It offers the ability to make accurate thickness and refractive index measurements with high resolution. Over the years, it has also been demonstrated to be a powerful technique for optical waveguides characterization. Fig. 1a shows the schematic plot of the prism coupling measurement. In most cases, a laser beam striking the prism is normally totally reflected at the prism base onto a detector. Especially, when the incident angles are at certain discrete values, the light can tunnel across the air gap into the guiding region through the optical propagation mode coupling, resulting in a sharp dip in the intensity of the incident light reaching the detector which is referred to the dark-mode spectrum. Furthermore, the mode numbers, the mode effective refractive indices, as well as the mode types can be determined with respect to the mode plots. Fig. 1b shows the dark-mode spectra of Nd:YLF planar waveguides irradiated

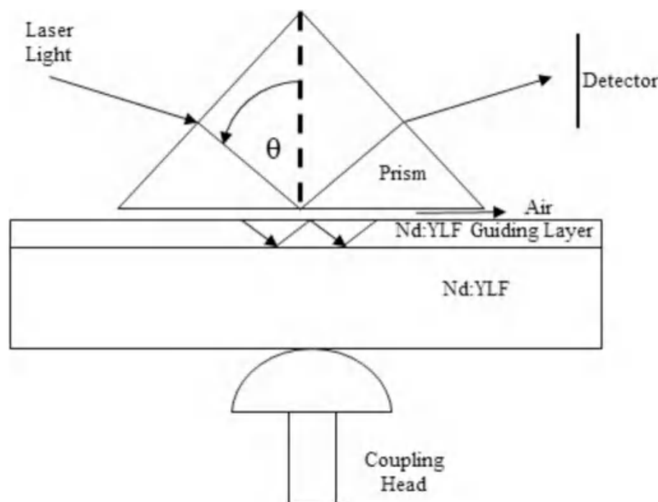

Fig. 1. (a) Schematic of the measurement mechanism of prism coupling method; **(b)** mode plots of the reflected light at a wavelength of 632.8 nm with TE polarization for 4.5-MeV Si-irradiated Nd:YLF.

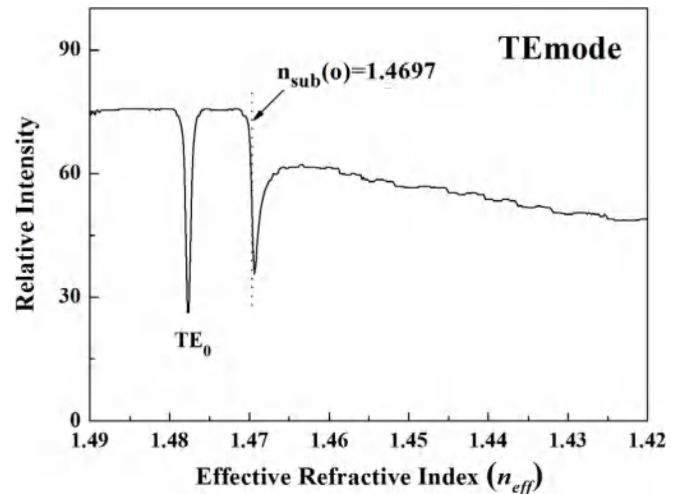

Fig. 1. (*continued*)

by 4.5-MeV-Si ions at fluences of $1.0 \times 10^{14}\,cm^{-2}$, which were recorded by a Model 2010 prism coupler at a wavelength of 632.8 nm. The ordinary refractive index of pristine Nd:YLF crystal (n_{sub} = 1.4697) is also given for comparison. As indicated in Fig. 1b, when the laser beam is employed with TE polarization, one narrow and sharp drop is detected. It should be pointed out that the detectable TE mode is confined by the n_0-enhanced region because of the higher mode effective index comparable with the pristine crystal. According to previous researches, several factors are assumed to be responsible for the refractive index change in implanted crystals, including spontaneous polarization, molar polarization, and molar volume, which could be directly influenced by ion implantation process [21,23,24]. It is well-known that there are two factors dominating the lattice damage in the crystal, the electronic ionizations and the nuclear collisions. In near surface, the electronic interaction induced damage component is responsible for an increase in the refractive index; on the contrary, the other damage component produced by nuclear collision cascade causes lowering of the refractive index [25,26]. Despite these impressive advances, the actual index-raised mechanism of implantation is not completely understood; further research will be carried on.

Since the profile of refractive index is of great importance for characterizing waveguide, different methods have been developed to fit the refractive index profile from the measured experimental modes, such as the inverse Wentzel–Kramers–Brillouin method (WKB) [27], parameterized index profile reconstruction (PIPR) [28], the intensity calculation method (ICM) [29] and RCM. Here, RCM developed by Chandler and Lama was chosen to reconstruct the refractive index profile of Si-ion-implanted Nd:YLF waveguide because it has been proven to be remarkably successful for characterizing the refractive index profiles of ion-implanted waveguide. For the first step, a conceivable profile is assumed, which is characterized by a set of parameters, including the basic shapes of the profile, the indices of the barriers, sample surfaces and substrate, the location of barrier inside the crystals, etc.; then this profile is used to calculate the effective refractive index of each mode by using RCM; finally, adjust certain parameters to alter the refractive index profile until the calculated effective refractive indices match the measured ones with the satisfied error. With these parameters, such a profile is supposed to approximately depict the refractive index behavior in the waveguides. Fig. 2 shows the reconstructed ordinary refractive index profile of Nd:YLF waveguide formed by the 4.5-MeV-Si implantation with fluences of $1.0 \times 10^{14}\,cm^{-2}$ based on RCM. As one can see that an enhanced well with a positive index change of ~2.06% is created from the near surface region of the sample, whilst a narrow optical barrier with a lower refractive index is built up at a depth of ~2.4 μm which acts as the

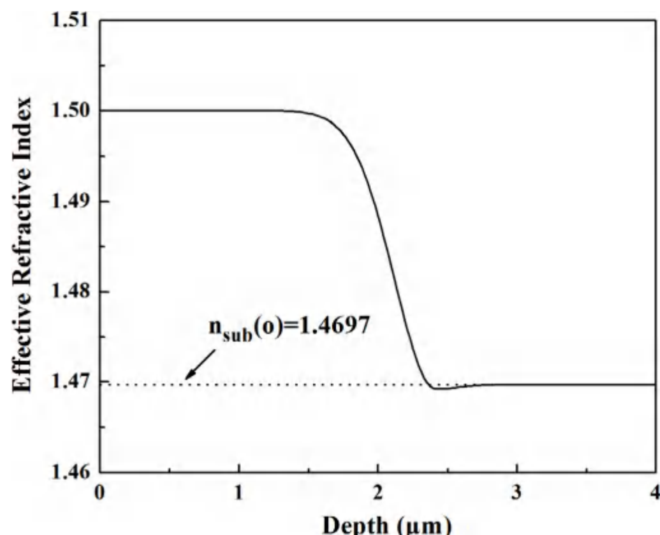

Fig. 2. Reconstructed refractive index profile of Nd:YLF waveguide formed by the 4.5-MeV-Si implantation at fluences of $1.0 \times 10^{14}\,cm^{-2}$ at 632.8 nm.

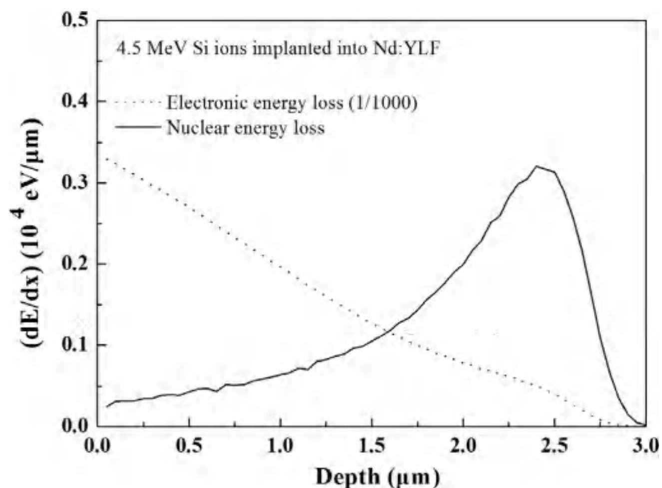

Fig. 4. Nuclear and electronic energy losses as a function of penetration depth for 4.5 MeV Si ions implanted into Nd:YLF crystal based on SRIM code.

guiding region confining the light propagation in relevant mode. It is also found that the measured effective refractive index (1.4777) agrees with the calculated value (1.4773) better than 10^{-3}. The difference is within the error range.

Based on the reconstructed refractive index profile shown in Fig. 2, a modal analysis on the measured TE mode is also performed to investigate the light propagation property in the Si-implanted Nd:YLF waveguide. Fig. 3 depicts the field intensity distribution of TE mode for the Nd:YLF waveguide fabricated by 4.5 MeV Si ions implantation at doses of $1.0 \times 10^{14}\,cm^{-2}$. It can be observed that the field of fundamental TE_0 is relatively well confined within the guide region. The result indicates the light confinement can be achieved in Nd:YLF crystal through 4.5 MeV Si ions implantation at doses of $1.0 \times 10^{14}\,cm^{-2}$. This also implies that the implantation condition we selected could be a promising candidate for construction of single-mode waveguide devices in Nd:YLF crystal.

Damage induced by implantation played an important role in the formation of waveguides because it produces a significant change in the refractive indices of most materials. Normally, there are two different types of damage produced in energetic ion implantation processes, which is dominated by two regimes, i.e. the electronic ionizations and the nuclear collisions cascade. The software Stopping and Range of Ions in Matter (SRIM 2013) were used to simulated the process of 4.5-MeV-Si implantation into Nd:YLF crystal. Fig. 4 shows the simulated the damage distributions as a function of penetration depth according to the code SRIM 2013. It is seen that the electronic damage takes place mainly during the trajectory of incident ions generating color centers and near-surface damage, whilst the nuclear damage of the Nd:YLF crystal is concentrated at the end of the Si ion track. The location of the peak value of the nuclear energy deposition is at a depth of ~2.4 μm, which is in agreement with the depth of the optical barrier in the refractive index profile.

In order to obtain a better understanding of the Nd:YLF crystal luminescence property changes induced by the Si ion implantation, the room temperature UC and NIR PL emission spectra from both the Si-implanted and pristine samples were performed upon excitation by an 808-nm laser. Fig. 5 depicts the emission profiles of green and yellow up-conversion in the Si-implanted sample and pristine Nd:YLF crystal. In both cases, there appears two emission bands in the green and yellow region locating at 518–542 nm and 578–602 nm corresponding to the $^4G_{7/2} \rightarrow {}^4I_{9/2}$ and $^4G_{7/2} \rightarrow {}^4I_{11/2}$ ($^4G_{5/2} \rightarrow {}^4I_{9/2}$) transitions of Nd^{3+} ions, respectively [30,31]. The relatively strong emission peaks are centered at 530, 588 and 595 nm, respectively. Note that the spectra recorded for both pristine and Si-implanted samples show similar

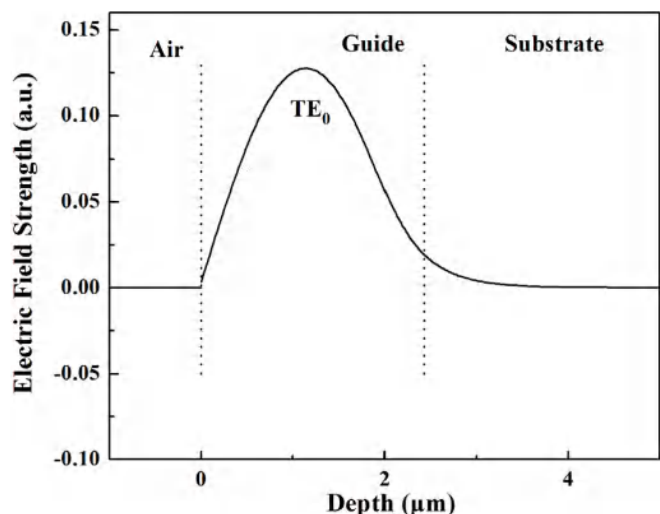

Fig. 3. Field intensity distribution of TE mode for the Nd:YLF waveguide formed by 4.5 MeV Si ions implantation at doses of $1.0 \times 10^{14}\,cm^{-2}$.

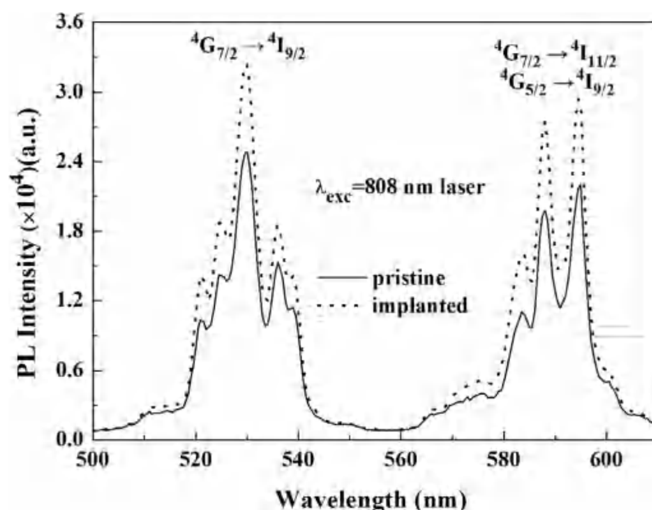

Fig. 5. The UC emission spectra of both pristine and implanted samples upon 808-nm laser excitation.

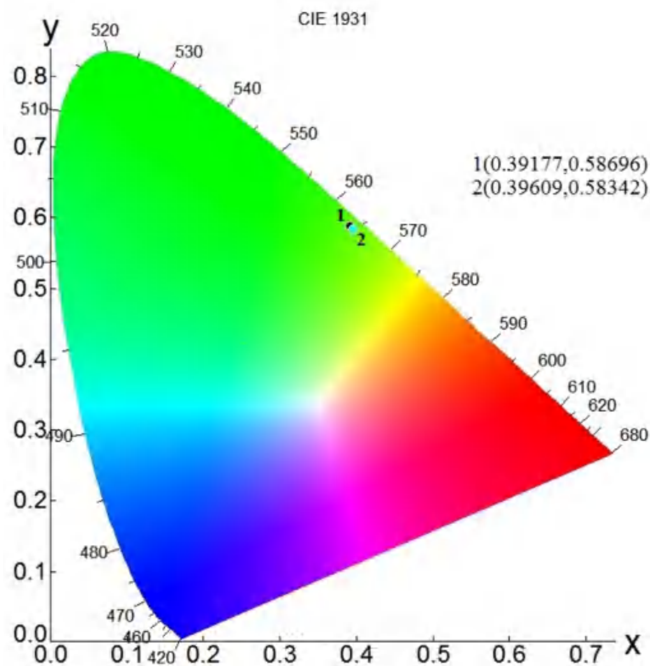

Fig. 6. CIE chromaticity diagram of both pristine (black dot 1) and implanted (blue dot 2) samples.

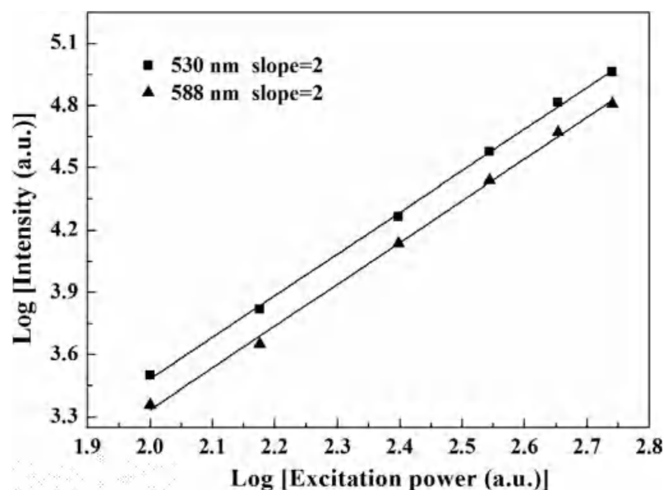

Fig. 7. Pump power dependence of UC emissions in the Si-implanted Nd:YLF crystal.

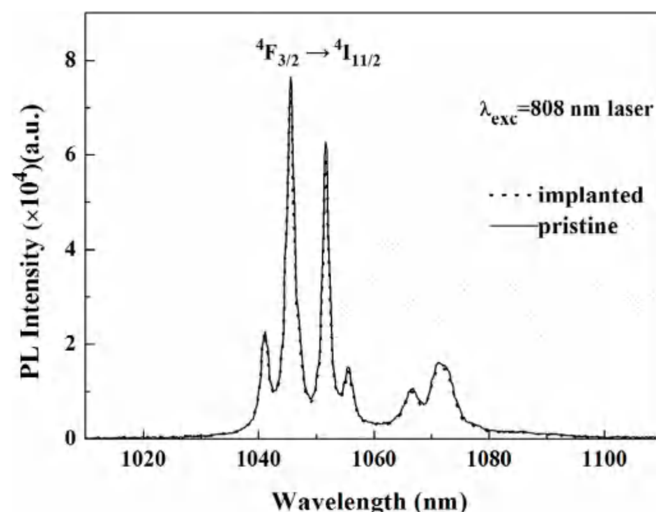

Fig. 8. The NIR emission spectra of both pristine and implanted samples under 808-nm laser excitation.

features except the change in intensities of the UC emission bands. As we can see, the fluorescent intensities increase after Si ions implantation. In details, for UC emission centered at 530, 588 and 595 nm, the fluorescent intensities from the Si-implanted sample increase by 30.3%, 38.6% and 31.7% in comparison to the pristine sample. It should be noted that there are several typical uncertainties in fluorescent intensity detection, such as instrument and sample-related factors. Although the power of diode laser varies during the measurements, the power stability of the diode laser used in the measurement is below than 5%, which is much smaller than the intensity difference between the achieved spectra. One can therefore conclude that the enhanced UC fluorescent intensity in the implanted sample is due to the Si ions implantation. Hence, the results indicate that Si ions implantation allows the fabrication of optical waveguides in Nd:YLF crystals increasing the UC fluorescent intensity of active Nd^{3+} ions in the pristine crystal. The chromaticity Commission International I'Eclairage (CIE) coordinates of the Nd^{3+} fluorescence of the pristine and Si-implanted Nd:YLF crystals are also shown in Fig. 6, corresponding to the black dot 1 and blue dot 2. The color coordinates of those two dots are also labeled. As one can see that the two spots almost overlap on the CIE map.

The excitation power dependences of the UC emission intensities helps in identifying the number of photons involved and the excitation mechanisms responsible for the UC emission to occur. During the UC emission process, the emission intensity (I) is proportional to the nth power of the pump intensity (P) as the following relation [32]:

$$I \propto P^n \tag{1}$$

where n is the number of pumping photons and can be fitted from the slope of the log$I$-log$P$ plot. Fig. 7 displays the double-logarithmic plots of the excitation power dependent UC emission for the Si-implanted sample. The fitted slopes for those two UC emissions have the same values of 2.0 indicating that both UC emissions are owing to two-photon excitation process.

Fig. 8 shows the comparison of the near-infrared fluorescence emission spectra of Nd^{3+} gained from the Si-implanted sample and pristine Nd:YLF crystal. For both cases, the observed typical emission band of Nd^{3+} in the ranges of 1035–1097 nm is ascribed to $^4F_{3/2} \rightarrow {}^4I_{11/2}$ radiative transition, where the dominant emission lines are centered at 1045 nm and 1051 nm. In details, the dominate spectra bands consist of a set of peaks at 1041, 1045, 1051, 1055, 1066 and 1071 nm. As already known, the NIR emissions around 1064 nm of Nd^{3+} can be considered as the typical four-level lasing actions under 808-nm photons pumping. Herein the abundant 4*f* electronic configurations of Nd^{3+} ions can be split into much more stark sublevels due to the interaction between the Nd^{3+} ions and the crystal field of the hosts. Thus, the transitions between the stark energy levels will result in the multiple so-called satellite emission lines [33]. It is worth mentioning that the NIR emission spectra measured in the Si-implanted sample and pristine Nd:YLF crystal show similar luminescence signals in terms of both intensity and spectral shape. Therefore the original NIR features of Nd^{3+} can be well preserved after the implantation of 4.5 MeV Si ions at fluences of $1.0 \times 10^{14}\,cm^{-2}$.

4. Conclusion

In summary, the Nd:YLF optical planar waveguides were formed by 4.5-MeV Si ions implantation at fluences of $1.0 \times 10^{14}\,cm^{-2}$ at room temperature. The TE guiding modes were measured by the prism coupling technique at a wavelength of 632.8 nm. The results indicate that the Nd:YLF waveguides exhibit the "index-enhanced" characteristics. The refractive index profile of the Si-implanted Nd:YLF waveguide was

reconstructed. The performed modal analysis indicates that the field of TE mode can be well restricted in the guiding region. The spontaneous generations of UC and NIR fluorescence emissions are also investigated under excitation by an 808-nm laser diode. According to the PL measurements, the results indicate that the fluorescent features of Nd:YLF can be well preserved under irradiation by 4.5-MeV Si ions with fluences of $1.0 \times 10^{14}\text{cm}^{-2}$. In particular, the intensities of UC emissions in the implanted sample are higher than those obtained from the pristine Nd:YLF crystal. The pumping power dependence studies indicate that two-photon process is responsible for the UC luminescence. The fabricated structures are good candidates for the development of nonlinear integrated laser sources.

Acknowledgements

This work is supported by “the Fundamental Research Funds for the Central Universities” (Grant no. 2015XKMS083). The authors also thank the State Key Laboratory of Nuclear Physics and Technology of Peking University for the help with ion implantation.

References

[1] R. Moncorge, Ann. Chim. Sci. Mater. 28 (2003) 5–20.
[2] R.C. Botha, H.J. Strauss, C. Bollig, W. Koen, O. Collett, N.V. Kuleshov, M.J.D. Esser, W.L. Combrinck, H.M. Von Bergmann, Opt. Lett. 38 (2013) 980–982.
[3] B.M. Walsh, U. Hommerich, A. Yoshikawa, A. Toncelli, J. Lumin. 197 (2018) 349–353.
[4] T.Y. Dai, Z.G. Fan, J. Wu, Y.L. Ju, B.Q. Yao, Z.G. Zhang, K. Teng, X.G. Xu, X.M. Duan, Infrared Phys. Technol. 82 (2017) 40–43.
[5] P. Kroetz, A. Ruehl, K. Murari, H. Cankaya, F.X. Kärtner, I. Hartl, R.J.D. Miller, Opt. Express 24 (2016) 9905–9921.
[6] J. Dong, X.S. Liu, C. Peng, Y.Q. Liu, Z.Y. Wang, Appl. Sci. Basel. 5 (2015) 1837–1845.
[7] H.C. Liang, C.S. Wu, Opt. Express 25 (2017) 13697–13704.
[8] S. Xu, S.F. Gao, Mater. Lett. 183 (2016) 451–453.
[9] M. Chen, Z.C. Wang, B.S. Wang, F. Yang, G.C. Zhang, S.J. Zhang, F.F. Zhang, X.W. Zhang, N. Zong, Z.M. Wang, Y. Bo, Q.J. Peng, D.F. Cui, Y.C. Wu, Z.Y. Xu, J. Lumin. 172 (2016) 254–257.
[10] J.M. Lv, X.T. Hao, F. Chen, Opt. Express 24 (2016) 25482–25490.
[11] I. Bányász, Z. Zolnai, M. Fried, S. Berneschi, S. Pelli, G. Nunzi-Conti, Nucl. Instrum. Methods Phys. Res., Sect. B 326 (2014) 81–85.
[12] D.L. Zhang, J. Kang, Q. Zhang, W.J. Du, W.H. Wong, E.Y.B. Pun, Opt. Mater. Express 5 (2015) 1715–1721.
[13] M. Casale, D. Bucci, L. Bastard, J.E. Broquin, Ceram. Int. 41 (2015) 7466–7470.
[14] F. Chen, X.L. Wang, K.M. Wang, Opt. Mater. 29 (2007) 1523–1542.
[15] Y. Tan, F. Chen, L. Wang, Y. Jiao, Nucl. Instrum. Methods Phys. Res., Sect. B 260 (2007) 567–570.
[16] B.X. Xiang, Y.J. Ma, H.P. Han, M. Wang, H. Zhang, S.C. Ruan, Opt. Mater. Express 7 (2017) 1794–1803.
[17] B.X. Xiang, L. Wang, Jpn. J. Appl. Phys. 56 (2017) 050306.
[18] G. Fu, K.M. Wang, X.L. Wang, F. Lu, Q.M. Lu, D.Y. Shen, H.J. Ma, R. Nie, Surf. Coat. Technol. 201 (2007) 5427–5430.
[19] Y. Liu, Q. Huang, M.L. Crespillo, M. Qiao, P. Liu, X.L. Wang, Opt. Mater. 64 (2017) 391–400.
[20] F. Chen, Laser Photon. Rev. 6 (2012) 622–640.
[21] Y.J. Ma, F. Lu, J.J. Yin, X.H. Liu, Opt. Eng. 52 (2013) 097101.
[22] P.J. Chandler, F.L. Lama, Opt. Acta 33 (1986) 127–143.
[23] Y. Jiang, K.M. Wang, X.L. Wang, F. Chen, C.L. Jia, L. Wang, Y. Jiao, Phys. Rev. B 75 (2007) 195101.
[24] J.J. Yin, F. Lu, X.B. Ming, Y.J. Ma, M.B. Huang, J. Appl. Phys. 108 (2010) 033105.
[25] G.G. Bentini, M. Bianconi, M. Chiarini, L. Correra, C. Sada, P. Mazzoldi, N. Argiolas, M. Bazzan, R. Guzzi, J. Appl. Phys. 92 (2002) 6477–6483.
[26] G.G. Bentini, M. Bianconi, L. Correra, M. Chiarini, P. Mazzoldi, C. Sada, N. Argiolas, M. Bazzan, R. Guzzi, J. Appl. Phys. 96 (2004) 242–247.
[27] J.M. White, P.F. Heidrich, Appl. Opt. 15 (1976) 151–155.
[28] D. Fluck, D.H. Jundt, P. Günter, M. Fleuster, Ch. Buchal, J. Appl. Phys. 74 (1993) 6023–6031.
[29] X.Z. Liu, F. Lu, F. Chen, Y. Tan, R. Zhang, H. Liu, L. Wang, L.L. Wang, Opt. Commun. 281 (2008) 1529–1533.
[30] D.S. da Silva, T.A.A. de Assumpcao, L.R.P. Kassab, C.B. de Araujo, J. Alloy. Comp. 586 (2014) S516–S519.
[31] M.H.A. Mhareb, S. Hashim, S.K. Ghoshal, Y.S.M. Alajerami, M.A. Saleh, R.S. Dawaud, N.A.B. Razak, S.A.B. Azizan, Opt. Mater. 37 (2014) 391–397.
[32] M. Pollnau, D.R. Gamelin, S.R. Luthi, H.U. Gudel, M.P. Hehlen, Phys. Rev. B 61 (2000) 3337–3346.
[33] H.Y. Shen, R.R. Zeng, Y.P. Zhou, G.F. Yu, C.H. Huang, Z.D. Zeng, W.J. Zhang, Q.J. Ye, IEEE J. Quant. Electron. 27 (1991) 2315–2318.